A New Series of Estrogen Receptor Modulators That Display Selectivity for Estrogen Receptor β

Brad R. Henke,*,† Thomas G. Consler,‡ Ning Go,§ Ron L. Hale,§,|| Dana R. Hohman,†,⊥ Stacey A. Jones,‡ Amy T. Lu,§,|| Linda B. Moore,‡ John T. Moore,‡ Lisa A. Orband-Miller,‡ R. Graham Robinett,‡ Jean Shearin,‡ Paul K. Spearing,† Eugene L. Stewart,‡ Philip S. Turnbull,‡ Susan L. Weaver,‡ Shawn P. Williams,‡ G. Bruce Wisely,‡ and Millard H. Lambert‡

GlaxoSmithKline Research and Development, Research Triangle Park, North Carolina, 27709, and Affymax Research Institute, Santa Clara, California 95051

Received July 8, 2002

A series of 1,3,5-triazine-based estrogen receptor (ER) modulators that are modestly selective for the ERβ subtype are reported. Compound **1**, which displayed modest potency and selectivity for ERβ vs ERα, was identified via high-throughput screening utilizing an ERβ SPA-based binding assay. Subsequent analogue preparation resulted in the identification of compounds such as **21** and **43** that display 25- to 30-fold selectivity for ERβ with potencies in the 10−30 nM range. These compounds profile as full antagonists at ERβ and weak partial agonists at ERα in a cell-based reporter gene assay. In addition, the X-ray crystal structure of compound **15** complexed with the ligand binding domain of ERβ has been solved and was utilized in the design of more conformationally restrained analogues such as **31** in an attempt to increase selectivity for the ERβ subtype.

Introduction

Estrogen replacement therapy is currently one of the most effective treatments for menopausal symptoms such as hot flushes and urogenital atrophy and has also shown utility in the prevention and management of postmenopausal osteoporosis.[1] In addition, some existing data suggest that estrogens also exert beneficial effects on both the cardiovascular system and central nervous system, leading to a potential utility for estrogens in the treatment of atherosclerosis[2] and Alzheimer's disease.[3] Despite the beneficial effects of estrogens, there is evidence to suggest an increase in reproductive tissue cancer,[4,5] which leads to both a restriction of widespread use and long-term compliance issues. This liability has resulted in a large research effort within the scientific community devoted to the discovery of agents that can maintain the benefits of estrogens while avoiding the risks. Drugs such as raloxifene and tamoxifen (Figure 1) that have tissue-selective estrogen agonist or antagonist effects are examples of such agents that hold the promise of a safer alternative to estrogen.[6,7] There continues to be a tremendous amount of effort to understand the molecular basis for the tissues-specific effects of these "anti-estrogens",[8] which are now commonly referred to as selective estrogen receptor modulators (SERMs).

Estrogens exert most of their biological effects via interaction with the estrogen receptor (ER), a member of the nuclear hormone receptor superfamily. These receptors are ligand-activated transcription factors that couple the interaction with their cognate hormones to the modulation of gene expression. Until recently estrogen signaling was thought to occur through a single nuclear receptor. However, the discovery in 1996 of a second ER subtype, termed ERβ,[9,10] has increased the level of complexity of estrogen signaling. The two receptor subtypes (ERα and ERβ) show significant sequence homology in their DNA and ligand binding domains; however, they exhibit differences in their tissue distribution patterns, ligand selectivity, and transcriptional properties.[11,12] Additionally, studies with receptor subtype specific knockout mice[13,14] and double-knockout mice[15] suggest that the two ER subtypes may have distinct biological roles.

While these studies with knockout mice have provided some understanding of the differential pharmacology exhibited by ERα and ERβ, the availability of subtype-selective ligands would greatly assist in probing the pharmacology associated with the two receptor subtypes. The comparative binding affinities and functional responses at ERα and ERβ for a number of steroidal and nonsteroidal estrogens have been reported.[12,16−19] These studies reveal that most of the estrogens tested bind to both ER subtypes with very similar affinity, usually within the range of 10-fold binding selectivity for a given receptor subtype. This is not surprising in light of the high degree of homology between the amino acid residues lining the ligand binding domains (LBDs) of ERα and ERβ.[12] Interestingly, there have been observed differences in both potency and response (agonist vs antagonist) in cell-based transcriptional assays with several steroidal and nonsteroidal estrogen ligands,[16,20] which suggests it may be possible to develop functionally subtype-selective estrogen receptor modulators. Indeed, functional selectivity of greater than 100-fold for ERα has been observed with certain ligands.[20]

* To whom correspondence should be addressed. Address: GlaxoSmithKline, NTH-M1413, Five Moore Drive, Research Triangle Park, NC 27709-3398. Phone: (919) 483-1363. Fax: (919) 315-0430. E-mail: brh14990@gsk.com.
† Metabolic and Viral Diseases Drug Discovery, GlaxoSmithKline.
‡ Discovery Research, GlaxoSmithKline.
§ Affymax Research Institute.
|| Current Address: Alexza Corp., Mountain View, CA 94040.
⊥ Current Address: Eli Lilly & Co., Indianapolis, IN 46285.

10.1021/jm020291h CCC: $22.00
Published on Web 10/26/2002

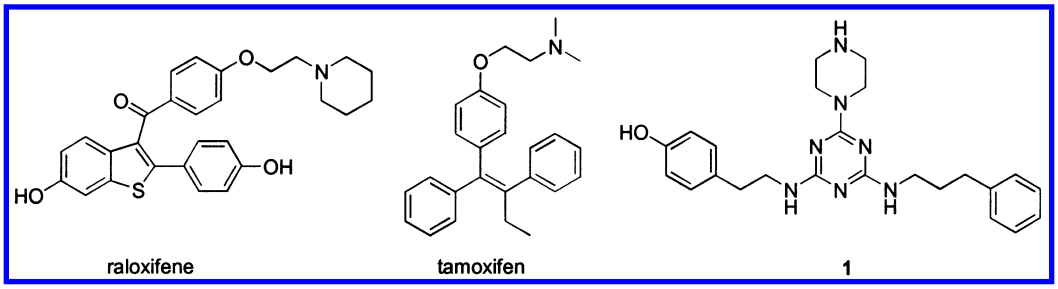

Figure 1. Estrogen receptor ligands.

Scheme 1[a]

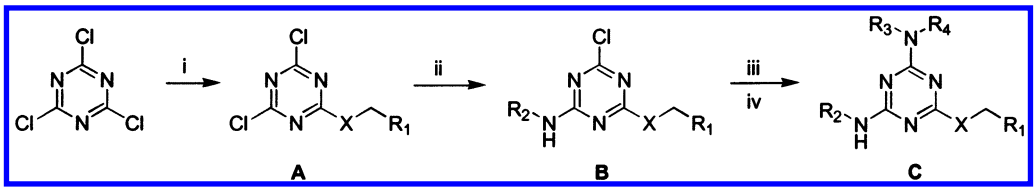

[a] Reagents: (i) R_1CH_2X, *N*,*N*′-diisopropylethylamine or Proton Sponge, DCM, −20 to 0 °C, 2 h, (ii) R_2NH_2, *N*,*N*′-diisopropylethylamine, DMF or THF, room temp, 4 h; (iii) R_3R_4NH, 2-propanol, CH_3CN, or CH_3CN/DMF, reflux, 18 h; (iv) 4 N HCl, 1,4 dioxane, room temp, 18 h (if necessary).

However, potent and highly selective ligands for ERβ have remained fairly elusive. Selectivities on the order of 10-fold have been reported for certain phytoestrogens such as genistein and in a series of arylbenzthiophenes.[21] Notably, a recent report from Katzenellenbogen disclosed compounds with up to 70-fold higher relative binding affinity for ERβ.[22] Importantly, all of these ERβ-selective ligands profile as agonists in functional assays; we are unaware of any reports in the literature to date describing ERβ-selective functional antagonists.

To develop a greater understanding of the pharmacology associated with subtype-selective modulation of ERβ, we initiated a program to identify compounds that show a high degree of selectivity for ERβ. A high-throughput binding assay was developed to identify ligands capable of binding to ERβ. Using this assay, we identified a novel triazine-derived ER ligand (**1**, Figure 1) that showed modest selectivity for ERβ. In this paper we report the medicinal chemistry efforts to improve the potency and ERβ selectivity of this hit and in vitro biological activity for this series of ER modulators. In addition, we describe the X-ray crystal structure of a member of this series (compound **15**) complexed with the LBD of ERβ and we describe our efforts utilizing both this structure and molecular modeling to design ERβ-selective ligands.

Chemistry

Compounds found in Tables 1−3 were synthesized via the general route depicted in Scheme 1. Addition of 1 equiv of the requisite amine, thiol, or alcohol to cyanuric chloride in dichloromethane at −20 to 0 °C in the presence of 1 equiv of base afforded adduct **A** in which a single chlorine has been displaced. Subsequent reaction of this adduct with 1 equiv of the second nucleophile at room temperature in acetonitrile or THF afforded disubstituted adduct **B**. The final substituent was introduced by reaction with an excess of the appropriate amine nucleophile in refluxing 2-propanol, acetonitrile, or acetonitrile/DMF mixtures. We found that addition of substituents containing a phenol moiety to cyanuric chloride resulted in formation of byproducts via competing nucleophilic addition of the free phenol; hence, the phenol-containing substituent was introduced either second or last. Apparently the reduced reactivity of the mono- and dichlorotriazines **A** and **B** is sufficient to suppress competing phenol addition in the presence of the more nucelophilic sulfur and amine moieties. In addition, often the first two addition reactions were clean enough that the intermediates **A** and **B** were carried on directly into the final addition reaction upon simple workup without rigorous purification and characterization. Compounds from Table 3 where the substituted piperazine was not commercially available were prepared by reacting BOC-piperazine with intermediate **A** or **B**, followed by addition of the third nucleophile (if necessary), deprotection with 4 M HCl in 1,4-dioxane, and subsequent alkylation (analogues **35**, **38**, **40**−**47**), acylation (analogues **48**−**53**), or sulfonylation (analogues **54**−**56**) with the appropriate electrophile. Most of these analogues were prepared via solution-phase chemistry; however, solid-phase array synthesis of analogues was also carried out via linkage of one of the amine substituents to either a photocleavable or acid-cleavable resin. The synthesis of 2,4,6-trisubstituted triazines on solid support has been reported by other groups;[23−25] our protocols were similar and will be reported in a separate publication. Synthetic routes and procedures for preparation of the noncommercial amine and thiol nucleophiles utilized in the construction of final compounds are provided as Supporting Information.

Biological Evaluation

Three in vitro assays were utilized to evaluate ER binding affinity and functional activity. High-throughput screening for compounds able to bind ERβ was done utilizing a scintillation proximity assay (SPA) with purified human ERβ LBD, using [^{3}H]-17β-estradiol as the radioligand. Details of the expression and purification of the ERβ protein are reported in the Experimental Section. Details of the assay development and data analysis are similar to previously reported SPA assays from our group.[26] Attempts to obtain sufficient quanti-

ties of purified human ERα LBD in order to set up a similar binding assay were unsuccessful. Therefore, binding assays using crude ERα and ER*β* proteins were developed in order to make more meaningful ligand affinity comparisons of the two receptors. Analogues prepared from medicinal chemistry efforts were tested for their ability to bind to crude ERα and ER*β* via a scintillation proximity assay using a bacterial lysate containing overexpressed GST-hERα or GST-hER*β* LBD, again using [^{3}H]-17*β*-estradiol as the radioligand. The functional profiles of selected compounds were evaluated in a transient transfection assay utilizing a human breast carcinoma cell line (T47D) transfected with expression vectors containing full-length hERα or hER*β*, *β*-galactosidase, and an estrogen-responsive reporter gene construct. Details of this assay are reported in the Experimental Section.

Results and Discussion

The ER binds a wide range of steroidal and nonsteroidal ligands with moderate to high affinity, with a minimal requirement of at least one para-monosubstituted phenol as the basic pharmacophore. The structural diversity of nonsteroidal estrogens having affinity for the ER is remarkable, with a number of chemically distinct templates reported as ER ligands.[6,7,22,27−36] A fairly detailed understanding of the binding requirements and the mode of action of steroidal and nonsteroidal ER ligands has been developed through the use of molecular modeling, receptor sequence analysis, and X-ray crystallographic analysis of agonist- and antagonist-bound ERα and ER*β*.[37−43] X-ray structures of ERα bound to estradiol[38,42] show that the A-ring hydroxyl group makes hydrogen bonds with Arg394 and Glu353, while the D-ring hydroxyl makes a single hydrogen bond with His524. The A-ring hydroxyl group fits optimally into the gap between Arg394 and Glu353, accepting a hydrogen bond from the arginine and donating a hydrogen bond to the glutamate. Arg394 and Glu353 effectively clamp the hydroxyl group in an orientation that places the phenol benzene ring between Phe404 and Leu387, where its planar geometry fits well. By contrast, the interaction with His524 is less demanding, since the hydrogen bonding group could act as either a donor or acceptor and can approach the histidine from different angles. X-ray structures of ERα bound to the nonsteriodal estrogens raloxifene,[38] diethylstilbestrol (DES), and 4-hydroxytamoxifen[43] reveal a similar pattern where the phenols that correspond to the A-ring phenol in estradiol are positioned precisely between Arg394 and Glu353 in each case, while the corresponding "D-ring" hydroxyl can be repositioned, as in raloxifene and DES, or omitted altogether, as in 4-hydroxytamoxifen. The ligand binding pocket in ERα has a total volume of 450 Å^3, which is considerably larger than the volume of estradiol, which is only 245 Å^3.[38] Thus, while a phenol group appears to be a key moiety for achieving strong binding to ERα, a precise fit to pocket is evidently not required, consistent with the wide range of steroidal and nonsteroidal compounds showing affinity for the ER.

Whereas estradiol and DES function as agonists at ERα as judged by cell-based reporter gene assays, raloxifene and tamoxifen are functional antagonists at ERα in these same assay systems. These antagonists contain side chains with a basic amine group (Figure 1). In each case, the basic amine group lies near Asp351, making a strong hydrogen bond in the raloxifene structure and a weaker hydrogen bond in the tamoxifen structure. The X-ray structures of ERα with raloxifene[38] and tamoxifen[43] revealed that these side chains protrude into volume that is occupied by the C-terminal AF2 helix in the agonist structures. On the basis of the structural data to date, the hypothesis put forth to explain the molecular basis of antagonism at ERα is that the basic side chains present in these antagonists effectively displace the AF2 helix out of a conformation that facilitates the recruitment of transcriptional coactivators and into an alternative conformation that does not recruit coactivators.[43]

The 530-residue ER*β* sequence is approximately 50% identical to the full-length 595-residue ERα sequence, with 97% identity in the 66-residue DNA binding domain (DBD) and 61% identity in the 236-residue LBD, where in this comparison the LBD was defined to exclude the nonconserved C-terminal tails of the F domain. The sequence identity is considerably higher than 61% in the ligand binding pocket, consistent with the fact the both ERα and ER*β* recognize estradiol and other estrogenic ligands. In the ERα/estradiol X-ray structure, only two of the residues within 5 Å of estradiol are different in ER*β*. These residues are ERα Leu384 in helix-5, which corresponds to Met336 in ER*β*, and ERα Met421 in helix-7, which corresponds to Ile373 in ER*β*. These residues lie roughly above and below the plane of ER-bound estradiol (i.e., on the *β*- and α-faces of the steroid), respectively. Initial modeling work, based on the published X-ray structures of ERα, suggested that the mutation of Met421 to isoleucine would open a methylene-sized hole in the ER*β* ligand binding pocket, near the α-face of the D ring of estradiol. In principle, a ligand that occupied this volume might be selective for ER*β*, since it would be expected to make repulsive contacts with Met421 in ERα. By contrast, the mutation of Leu384 to methionine in ER*β* would effectively close a methylene-sized pocket that exists in ERα near the *β*-face of the C and D rings of estradiol. A ligand that occupied this volume might show selectivity for ERα. Alternatively, in each case these selectivity effects could be reversed by making favorable stereoelectronic interactions with the methionine side chain. The modest change in both the steric and stereoelectronic nature of these two mutations suggests that highly selective agents might not be achieved simply by targeting of these two residues alone or in concert. In addition, ERα appears to be highly mobile,[43] and small conformational adjustments in the protein could compensate for the mutations, rendering the ERα and ER*β* pockets virtually indistinguishable.

Triazine **1** emerged from a high-throughput screen of our compound collection as having submicromolar affinity for ER*β*. Interestingly, structurally related *s*-triazine herbicides such as atrazine, simazine, and propazine have been studied for their endocrine-disruptive and tumor-promoting properties, which appear to be xenoestrogenic in their nature. However, these molecules have no affinity for the estrogen receptor in vitro[44] and recent studies suggest that their estrogenic

Table 1. In Vitro Binding of ER Ligands **1**−**8**

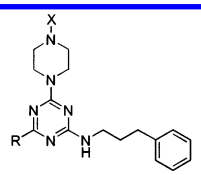

No.	R[a]	X	ER Binding: ERα K_i (nM)[b]	ER Binding: ERβ K_i (nM)[b]	β Sel.[c]
1	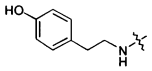	H	1380 ± 550 (11)	200 ± 110 (14)	7
2	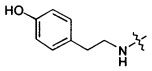	CH_3	3240 ± 80 (2)	490 ± 90 (2)	7
3	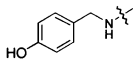	CH_3	5130 (1)	3690 (1)	1.5
4	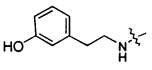	CH_3	> 10,000 (2)	4245 ± 350 (2)	N/A
5	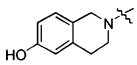	CH_3	>10,000 (2)	>10,000 (3)	N/A
6	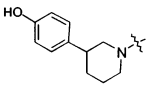	CH_3	>10,000 (2)	>10,000 (2)	N/A
7	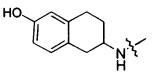	CH_3	1,000 ± 180 (6)	170 ± 20 (6)	6
8	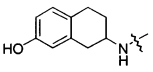	CH_3	>10,000 (2)	>10,000 (2)	N/A

[a] See figure. [b] The values for K_i were obtained from a least-squares fit of the concentration−response curves according to the equation $-b = -b_0/(1 + [L]/K_i)$ where b_0 is the counts bound in the absence of test compound and b is the counts bound in the presence of test compound at concentration [L] ± standard deviation (number of determinations). [c] Selectivity reported as K_i(ERα)/K_i(ERβ). N/A = selectivity not able to be accurately determined under assay conditions used.

effects are a result of induction of aromatase, the rate-limiting enzyme in the conversion of steriodal androgens to estrogens, rather than via direct interaction with ER.[45,46] Resynthesis and testing against both ER subtypes confirmed the affinity for ERβ at 200 nM (Table 1) and revealed a modest binding selectivity of approximately 7-fold for ERβ over ERα. We then systematically explored the three substituents off the central triazine core in an attempt to increase the potency and selectivity for ERβ. Structure−activity relationships for these two parameters were developed and pursued primarily on the basis of binding affinities for the two ER subtypes rather than on activity of compounds in the cell-based functional assay. Interpretations of potency can be complicated in the latter assay because of compound differences in cell penetration, metabolism, and potential differences in the ability of the two ER subtypes to interact with coactivator or corepressor proteins.[47]

Table 1 outlines the structure−activity relationships of the tyramine substituent attached to the triazine core of lead compound **1**. Aside from **1**, all of the analogues in Table 1 have an *N*-methylpiperazine group rather than a free N−H piperazine at the third point off the triazine core. However, comparison of **1** vs **2** (Table 1) and **17** vs **34** (Tables 2 and 3) suggests that methylation has only a minor effect on potency at either receptor subtype. Removal of one methylene unit in the chain (compound **3**, Table 1) led to >10-fold decrease in binding affinity at both receptor subtypes. A similar decrease in affinity was observed when the hydroxyl moiety was moved to the meta position (compound **4**) relative to the side chain. This loss of affinity upon repositioning of the phenol moiety is consistent with structure activity relationships reported in other nonsteroidal templates.[48,49] Various ring-constrained analogues (**5**−**8**) of the aminoethyl side chain provided no increase in ERβ affinity or selectivity; in fact, compound **7** was the only analogue to retain any activity at either ER subtype, showing potency and selectivity equal to **1**. This limited dataset suggested that this side chain prefers to be in a partially extended conformation with

the nitrogen atom out of the plane of the phenyl ring when bound to ER. Since the tyramine moiety was clearly mimicking the A ring of estradiol and structural data comparison of the two ER subtypes suggested little opportunity within this region of the LBD for achieving improved ERβ selectivity, we chose to abandon any further efforts in this region of the molecule.

The structure−activity relationships that evolved around the phenylpropylamino side chain of **1** are detailed in Table 2. Initially we focused on the aminopropyl portion of this substituent. Increasing the chain length by one methylene unit to butyl (compound **9**) completely eroded ERβ selectivity, primarily through an increase in affinity for ERα. Decreasing chain length to ethyl also led to a loss of ERβ selectivity (compare **1** vs **10**) but in this case mainly via a loss of affinity for ERβ rather than an increase in affinity for ERα. Initial attempts at conformationally constraining the propyl side chain (compounds **11** and **12**) led to a considerable decrease in ER affinity. Replacement of the amino group with sulfur consistently led to a 2- to 4-fold increase in binding affinity at both ER subtypes (compare **1** vs **13**, **15** vs **16**, **18** vs **19** in Table 2). However, replacement with oxygen led to a decrease in affinity (compare **1** vs **14**). Replacement of the benzylic methylene with oxygen also led to a decrease in binding at both receptor subtypes (compare **18** vs **15**, **19** vs **17**) with the greater loss appearing to be at ERβ, which resulted in a small loss of the desired ERβ selectivity. Interestingly, methylation of the amine nitrogen led to a modest but reproducible improvement in ERβ selectivity (compare **16** vs **17**), providing compound **17**, which was now 20-fold selective with an affinity of 15 nM at ERβ. Introduction of a group larger than methyl at this position led to a decrease in both affinity and selectivity for ERβ (compare entries **17** and **20**).

We also briefly explored the effects that phenyl ring substituents had on ER affinity. Electron-withdrawing groups such as chlorine or fluorine on the phenyl ring provided roughly 4-fold improvement in ER affinity at both receptor subtypes (compare **1** vs **16**, **13** vs **15**). The position of the substituent appears to have little effect on potency or selectivity (compare entries **17** vs **25**) as does the addition of a second electron-withdrawing group on the ring (compare entries **21** vs **24**, **17** vs **28**). Cyano and trifluoromethyl substituents appear to be slightly less effective in increasing ER affinity than simple halogens. Electron-donating substituents such as methyl are generally equipotent to the unsubstituted phenyl derivatives (compare entries **1** vs **26**). Finally, saturation of the phenyl ring (entry **29**) led to a loss in affinity at both receptor subtypes.

During our exploration of the structure−activity relationships of this series, we were able to obtain a cocrystal structure of the LBD of ERβ complexed with one of the triazine analogues, compound **15** (Figure 2). As expected, ERβ had the same overall fold as ERα. The phenol group of **15** makes hydogen bonds with Arg346 and Glu305, corresponding to the interactions with Arg394 and Glu353 in ERα. The piperazine ring of compound **15** protruded into the volume normally occupied by the AF2 helix, effectively displacing the AF2 helix into the coactivator binding groove. The outer (basic) nitrogen of the piperazine ring makes a hydrogen bond with ERβ Asp303, analogous to the hydrogen bond between the piperidine nitrogen of raloxifene and ERα Asp351. To facilitate comparison, the protein backbone of the ERβ/**15** structure was superimposed onto the backbones of the earlier ERα structures. This superimposition brought the phenol group of **15** into nearly perfect coincidence with the phenol group of estradiol and showed that the *p*-chlorophenyl ring corresponds roughly to the D ring of estradiol (Figure 3). The *p*-chlorophenyl ring fails to make any interaction with His475, corresponding to His524 in ERα. It does, however, fit against Ile373 in ERβ. This residue is mutated to Met421 in ERα, and the *p*-chlorophenyl ring would encounter some steric hindrance with the methionine sulfur if the triazine and methionine remained in the conformations observed in the ERβ structure and in the estradiol structure, respectively. This could provide a partial explanation for the ERβ selectivity, since the interactions with Ile373 in ERβ are expected to be more favorable than with Met421 in ERα. In addition, the amine and first methylene from the phenol arm of the triazine pack against Met336 in ERβ. This packing arrangement gives a modestly favorable interaction, particularly since the S−CH_3 dipole is oriented opposite the N−H dipole. By contrast, the more lipophilic leucine residue at this position in ERα would fail to make any favorable electrostatic interactions. During our work with the ERβ/**15** structure, reports of other ligand/ERβ crystal structures appeared in the literature[40] that were consistent with our structure, having the AF2 helix displaced into the coactivator-binding groove.

Detailed examination of the ERβ/**15** complex allowed us to rationalize some of the SAR we had observed thus far. Analysis of data for the ring-constrained compounds **5**−**8** had suggested that the linker was partially extended, with the nitrogen out of the plane of the phenyl ring. This was confirmed by the X-ray structure, and molecular modeling indicated that the (*R*)-enantiomer of aminotetrahydronaphthalenol derivative **7** overlaps well with the conformation of compound **15** seen in the X-ray structure. The crystal structure shows that the propylthio linker to the *p*-chlorophenyl ring of **15** adopts a highly twisted conformation that brings the phenyl ring back into the D-ring pocket. The constrained linker of **12** fails to turn the phenyl ring back into the pocket. The double bond of **11** corresponds to a bond in **15** that is rotated only 45° away from trans. Evidently, **11** can assume this general conformation but with a loss of potency corresponding to the redistributed conformational strain. The X-ray structure clearly shows space to accommodate a five-atom linker, as in **9**. The three-atom linker of **10** can turn the phenyl ring partially back into the pocket but leaves a significant empty void in the bottom of this pocket, which may account for the loss of potency relative to that of **1**. By contrast, the *p*-chlorophenylpropyl ring of **15** fills this pocket very well. The crystal structure shows that there is just barely enough space to accommodate a methyl group on the nitrogen, so it is not surprising that the ethyl substitution in **20** reduces the binding affinity relative to that seen with **17**. However, the X-ray structure does not explain some of the subtleties within the SAR. For example, it is not immediately clear why electron-

Table 2. In Vitro Binding of ER Ligands **9**−**31**

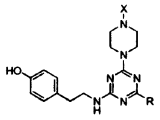

No.	R[a]	X	ER Binding ERα K_i (nM)[b]	ER Binding ERβ K_i (nM)[b]	β Sel.[c]
1	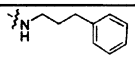	H	1380 ± 550 (11)	200 ± 110 (14)	7
9	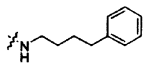	CH_3	415 ± 30 (2)	490 ± 220 (2)	0.8
10	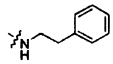	H	2370 ± 120 (3)	1750 ± 170 (3)	1.4
11	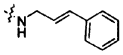	H	6870 ± 200 (2)	4200 ± 240 (2)	1.6
12		CH_3	>10,000 (2)	>10,000 (2)	N/A
13	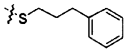	CH_3	270 ± 170 (8)	50 ± 20 (8)	5
14	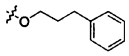	CH_3	2400 (1)	1000 (1)	2
15	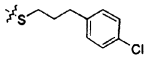	H	160 ± 170 (10)	15 ± 10 (10)	10
16	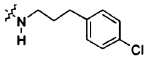	H	200 ± 50 (4)	55 ± 20 (4)	4
17	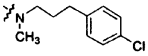	H	300 ± 120 (10)	15 ± 9 (10)	20
18	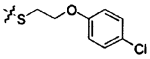	H	570 ± 60 (2)	90 ± 50 (2)	6
19	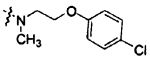	H	1000 ± 150 (2)	170 ± 30 (2)	6
20	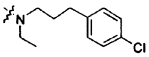	H	830 ± 170 (2)	100 ± 50 (2)	8
21	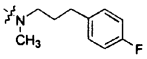	H	380 ± 100 (4)	15 ± 2 (4)	25
22	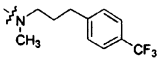	H	480 ± 80 (2)	75 ± 30(2)	6
23	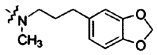	H	560 ± 150 (4)	30 ± 5 (4)	19
24	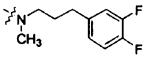	H	200 ± 5 (2)	20 ± 1 (2)	10
25	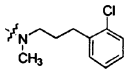	H	680 ± 290 (2)	40 ± 4 (2)	17
26	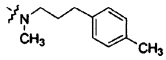	H	1140 ± 250 (2)	100 ± 15 (2)	11
27	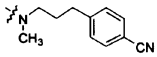	H	570 ± 90 (2)	90 ± 15 (2)	6
28	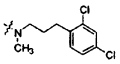	H	125 (2)	25 ± 8 (2)	5
29	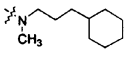	H	1420 ± 230 (2)	820 ± 380 (4)	2
30	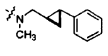	H	>10,000 (2)	1800 ± 270 (2)	N/A
31	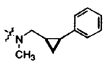	H	1240 ± 290 (6)	40 ± 15 (6)	31

[a] See figure. [b] The values for K_i were obtained from a least-squares fit of the concentration−response curves according to the equation $-b = -b_0/(1 + [L]/K_i)$ where b_0 is the counts bound in the absence of test compound and b isthe counts bound in the presence of test compound at concentration [L] ± standard deviation (number of determinations). [c] Selectivity reported as K_i(ERα)/K_i(ERβ). N/A = selectivity not able to be accurately determined under assay conditions used.

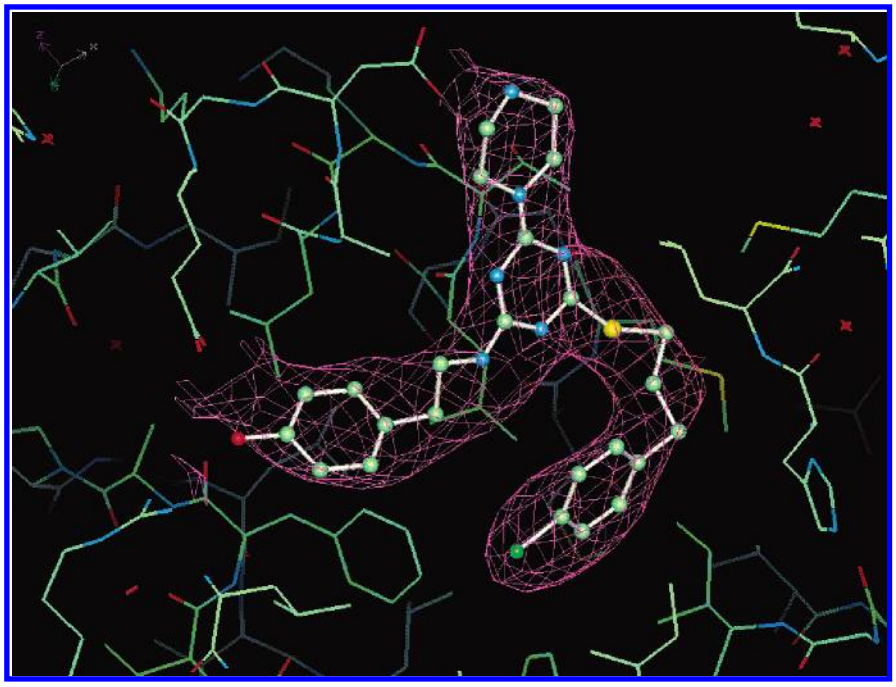

Figure 2. X-ray crystal structure of ERβ LBD/**15**. A σ-weighted $2F_o - F_c$ electron density map was contoured at 1.5σ, which allowed unambiguous placement of **15**.

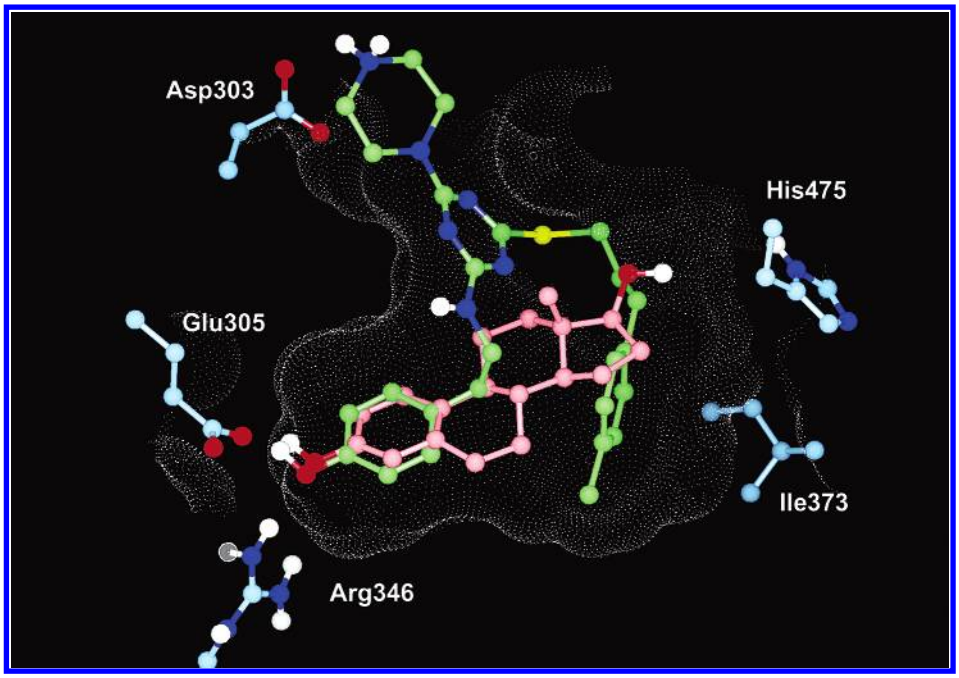

Figure 3. Binding modes of **15** and estradiol, showing selected side chains in ERβ. The ERα/estradiol X-ray structure[38] was overlaid onto the ERβ/**15** X-ray structure by superimposing backbone atoms in the core helices of the proteins. Carbon atoms are pale-blue in the ERβ protein, green in **15**, and pink in estradiol. Hydrogen, nitrogen, oxygen, and sulfur atoms are shown in white, blue, red, and yellow, respectively.

withdrawing groups on the phenyl ring tend to provide a modest enhancement of binding affinity, since the phenyl ring of **15** sits in a pocket that is entirely lipophilic.

While the initial straightforward attempts at conformationally constraining the phenylpropylamino side chain were unsuccessful (vide supra), the insight we had obtained from analysis of the ERβ LBD/**15** complex allowed us to revisit this topic. Docking calculations were carried out where the *p*-chlorophenylpropylthio side chain of **15** was replaced by several hundred different commercially available or "customized" primary amines. The *p*-chlorophenylpropylthio side chain was removed from the X-ray structure of **15** to give a "triazine core" within the ligand binding pocket for subsequent computational elaboration. The MVP program[50] attached each of the amines to the triazine core in turn, using a buildup procedure to "grow" the amine side chains into alternative low-energy conformations within the ERβ ligand binding pocket. The amines with the most favorable calculated binding energies were examined graphically using Insight-II[51] looking for features that might enhance the ERβ selectivity. This analysis suggested that placement of a *cis*-cyclopropyl

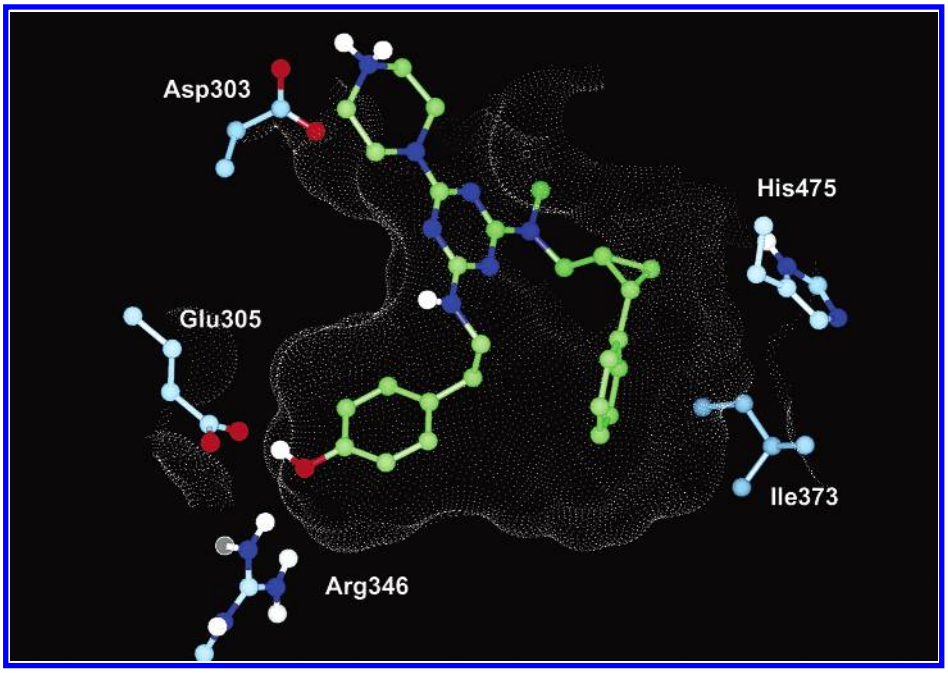

Figure 4. Predicted binding mode of **31**, showing selected side chains in ERβ. This shows the calculated binding mode of **31** having the lowest calculated energy. Carbon atoms are pale-blue in the ERβ protein and green in **31**. Hydrogen, nitrogen, oxygen, and sulfur atoms are shown in white, blue, red, and yellow, respectively.

group in the propyl chain as in compound **31** would help fix the linker in a conformation that directed the phenyl ring toward Ile373 in ERβ and into the volume occupied by Met421 in ERα. Compound **31** consistently displayed the highest selectivity (30-fold) for ERβ of any molecule within this series, while the corresponding *trans*-cyclopropyl compound **30,** which forces the phenylpropyl side chain into an extended conformation, was considerably less active at both receptor subtypes. However, the modest increase in selectivity observed with this molecule vs nonconformationally constrained analogues was disappointing. If our structural analysis is correct, then much of the subtype selectivity would depend on achieving a good fit in ERβ, while forcing the substituent into the volume normally occupied by Met421 in ERα. However, even with the cyclopropyl ring constraint, compound **31** still remains relatively flexible (Figure 4). We conclude that the conformational flexibility inherent in the basic structure of these ligands, the observed mobility of the two ER proteins, and the high degree of similarity in the ERα and ERβ ligand binding pockets conspire to fundamentally limit the ERβ selectivity that can be attained in this chemical series through structure-based drug design.

Table 3 lists compounds in which the piperazine moiety of **17** has been derivatized. Previous data on analogues generated by solid-phase library synthesis had indicated that acyclic amines at this position did not have good affinity for the ER (data not shown); hence, the more focused efforts were carried out with the piperazine as a point of diversity. A limited number of changes to the carbon framework of the piperazine were explored. Addition of methyl groups flanking the piperazine nitrogen eroded ERβ selectivity by increasing affinity for ERα (compare **17** vs **32** in Table 3), while the 2,5-diazabicyclo[2.2.1]heptane analogue **33** displayed approximately 5-fold lower affinity for both ER subtypes vs the parent piperazine. The X-ray structure of **15** reveals that the piperazine ring fits into the ERβ protein in a similar fashion to the piperidine ring of raloxifene in ERα,[38] protruding out of the ligand binding pocket and into the volume occupied by the AF2 helix in agonist-bound structures. The AF2 linker region, consisting of residues between helix-10 and the AF2 helix, packs loosely against the protein in the vicinity of the piperazine ring and adopts different conformations in ERα and ERβ. This linker region contains a single amino acid difference in the ER subtypes, where ERα Leu536 is mutated to ERβ Val487. Although the ERβ Val487 side chain lies only 6 Å from the piperazine ring of **15**, targeting this specific mutation is unlikely to achieve ERβ selectivity because evidence suggests the AF2 linker region can shift freely to accommodate changes in the ligand.

In general, derivatization of the piperazine nitrogen resulted in no benefit in terms of affinity or selectivity for ER. Compounds **34**−**47** are representative analogues obtained by alkylation of the piperazine nitrogen. Alkylation with simple alkyl groups (**34**−**36**) resulted in very little change in receptor affinity at ERβ, with the cyclopentyl derivative **36** displaying modestly reduced selectivity for ERβ. Direct attachment of a phenyl ring to the piperazine nitrogen as in compound **37** led to a 60-fold decrease in ERβ affinity vs compound **8**, while the corresponding benzyl derivative **38** is equipotent with **17**, suggesting that the basicity of this nitrogen is important for achieving good binding affinity. Inspection of the X-ray crystal structure reveals that this nitrogen makes a hydrogen bond interaction with Asp303 in ERβ, corresponding to Asp351 in ERα, which accounts for the observed SAR. Alkylation with heterocyclic compounds and other modestly polar groups containing hydrogen bond donor or acceptor groups (**39**−**47**) resulted in compounds with similar or slightly reduced binding affinity and selectivity for ERβ. Notably, both the hydroxyethyl analogue **39** and the thiazole analogue **43**

Table 3. In Vitro Binding of ER Ligands **32**−**56**

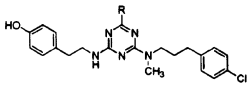

No.	R[a]	ER Binding ERα K_i (nM)[b]	ER Binding ERβ K_i (nM)[b]	β Sel.[c]
17	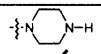	300 ± 120 (10)	15 ± 9 (10)	20
32		60 ± 15 (4)	15 ± 10 (4)	4
33		2275 ± 900 (6)	105 ± 30 (4)	22
34	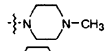	145 ± 3 (2)	15 ± 5 (2)	10
35	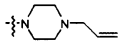	360 ± 130 (6)	30 ± 15 (6)	12
36	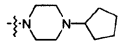	180 ± 50 (2)	40 (2)	5
37	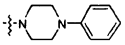	6320 ± 600 (2)	890 ± 60 (2)	7
38	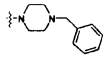	120 ± 5 (2)	8 ± 1 (2)	15
39	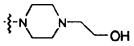	395 ± 175 (6)	15 ± 5 (6)	26
40	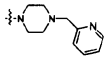	675 ± 190 (6)	50 ± 30 (6)	14
41	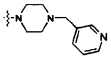	475 ± 215 (4)	35 ± 10(4)	14
42	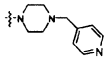	810 ± 120 (2)	115 ± 20 (2)	7
43	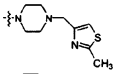	650 ± 400 (6)	25 ± 10 (6)	26
44	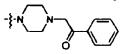	2040 ± 65 (2)	200 ± 65 (2)	10
45	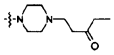	250 (2)	40 ± 15 (2)	6
46	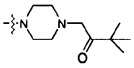	1025 ± 330 (2)	210 ± 150 (2)	5
47	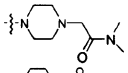	3000 ± 1900 (2)	270 ± 25 (2)	11
48	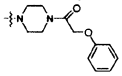	570 ± 170 (2)	100 ± 30 (2)	6
49	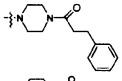	1050 ± 650 (2)	110 ± 30 (2)	10
50	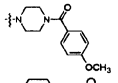	1130 ± 740 (4)	110 ± 60 (4)	10
51	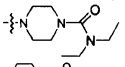	>10,000 (2)	790 (2)	N/A
52	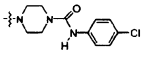	855 ± 260 (4)	425 ± 90 (4)	2
53	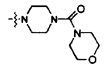	2360 ± (2)	400 (2)	6
54	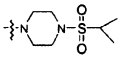	>10,000 (2)	600 ± 200 (2)	N/A
55	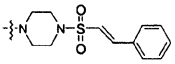	1300 ± 400 (2)	225 ± 35 (2)	6
56	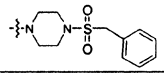	1450 ± 50 (2)	490 ± 125 (2)	3

[a] See figure. [b] The values for K_i were obtained from a least-squares fit of the concentration−response curves according to the equation $-b = -b_0/(1 + [L]/K_i)$ where b_0 is the the counts bound in the absence of test compound and b is the counts bound in the presence of test compound at concentration [L] ± standard deviation (number of determinations). [c] Selectivity reported as K_i(ERα)/K_i(ERβ). N/A = selectivity not able to be accurately determined under assay conditions used.

had binding profiles equal to that of **17**. Compounds **48**−**56** are representative analogues where the piperazine nitrogen has been acylated. In all cases, acylation resulted in a 5- to 40-fold loss of affinity at ERβ with a

Table 4. In Vitro Functional Activity of Selected ER Ligands

	ERα				ERβ				
compd	IC_{50} [a] (nM)	% inhib[b]	EC_{50} [c] (nM)	% act.[d]	IC_{50} [a] (nM)	% inhib[b]	EC_{50} [c] (nM)	% act.[d]	β sel[e]
17β-E2	IA	N/A	0.07 ± 0.9 (50)	100	IA	N/A	0.8 ± 2 (50)	100	0.08
raloxifene	0.7 ± 0.5 (10)	113 ± 8	IA	N/A	15 ± 10 (8)	120 ± 15	IA	N/A	0.05
15	80 ± 65 (5)	62 ± 22	160 ± 30 (4)	12 ± 1	6 ± 2 (6)	103 ± 6	IA (4)	N/A	13
17	110 ± 80 (4)	79 ± 4	180 ± 65 (4)	20 ± 4	5 ± 1 (4)	112 ± 5	IA (4)	N/A	20
21	240 ± 220 (5)	67 ± 3	200 ± 80 (4)	10 ± 2	15 ± 5 (4)	98 ± 5	IA (4)	N/A	16
31	565 ± 90 (2)	70 ± 1	500 ± 200 (2)	11 ± 5	20 ± 3 (2)	93 ± 2	IA (6)	N/A	28
39	30 ± 10 (4)	60 ± 2	180 ± 150 (4)	16 ± 6	15 ± 3 (4)	107 ± 7	IA (4)	N/A	2
43	150 ± 70 (4)	81 ± 4	150 ± 50 (4)	8 ± 3	5 ± 2 (4)	98 ± 2	IA (4)	N/A	30

[a] IC_{50}, the concentration of test compound required to inhibit 50% of the maximum alkaline phosphatase activity induced by 1 nM of 17β estradiol ± standard error (number of determinations). IA = inactive at 10^{-4} M. [b] % inhib, percent maximal inhibition by test compound of alkaline phosphatase activity stimulated by 1 nM 17β-estradiol treatment. [c] EC_{50}, the concentration of test compound required to induce 50% of the maximum alkaline phosphatase activity ± standard error (number of determinations). [d] % act, relative efficacy as determined by the percent of maximal alkaline phosphatase activity by test compound standardized to 17β-estradiol = 100%. [e] β sel, selectivity reported as IC_{50}(ERα)/IC_{50}(ERβ).

modest drop in selectivity. Since acylation reduces the basicity of the piperazine nitrogen, these results are consistent with those predicted on the basis of the structural information.

The functional profiles of some of the most potent and ERβ-selective analogues were evaluated in a cell-based (T47D) reporter gene transcription assay (Table 4). All of the triazine analogues profiled as antagonists at ERβ, achieving full inhibition of estradiol-stimulated reporter gene transcription equal in magnitude to that displayed by raloxifene, which also profiled as a full antagonist. Interestingly, these compounds profiled as weak partial agonists at ERα, activating the reporter gene with only 10−20% of the efficiency of estradiol. This partial agonism was confirmed by demonstration that these analogues can antagonize the effects of estradiol to a maximal extent of 60−80% when coadministered to these cells. Raloxifene showed no agonist activity at ERα in this assay, profiling as a full antagonist. This suggests the possibility that this series of compounds may modulate ER responsive genes in a manner different from that of both raloxifene and estradiol. In addition, the transcriptional potency of these compounds is in reasonable concordance with their binding affinities for both ER subtypes, and thus, the degree of ERβ selectivity seen in the binding assay is maintained in the cell-based environment. Compound **39** appears to be an exception to this correlation because a 10-fold increase in functional potency was observed when comparing antagonist potency to binding affinity on ERα. However, a direct correlation between ER binding affinity and functional potency is not always observed.[16,20,22] The origin of this discrepancy may be related to differences in cell penetration and/or metabolism, or factors outside of the ligand−receptor interaction such as differential receptor−cofactor interactions and differential use of the activation functions AF-1 and AF-2.

The ability of these ligands to fully antagonize ERβ while displaying partial agonist activity at ERα_is consistent with reports in the literature that indicate ERβ is more readily antagonized by a number of SERMs.[12,17] The structural basis for this difference in activity is not well understood. As mentioned previously, the origin of antagonism displayed by compounds such as raloxifene and tamoxifen is believed to result from the basic side chains of the molecules. These side chains effectively displace the AF2 helix out of the active position and into the coactivator binding groove, where it blocks the binding of coactivators.[43] Genistein, a partial agonist of ERβ, lacks a basic side chain and thus should permit the AF2 helix to fit into the same position in ERβ as is observed with estradiol and DES in ERα. However, in the X-ray structure of genistein bound to ERβ,[40] the AF2 helix is shifted into the coactivator groove. Compared with the structures of **15** and raloxifene in ERβ, the AF2 helix adopts the helical conformation over a greater length and sits more deeply in the groove, as permitted in the absence of any interfering side chain in the ligand. The (*R,R*)-enantiomer of a dialkyltetrahydrochrysene ER ligand has been reported to act as an agonist on ERα but as an antagonist on ERβ.[17] Crystal structures of this compound with ERα and ERβ reveal that it assumes slightly different orientations in the two binding sites and makes different interactions with His524 and His475 in helix-11, perhaps because of the mutation of Leu384 and Met421.[53] Like genistein, this compound lacks any protruding side chain and appears to achieve its antagonistic effect on ERβ through its failure to nucleate the interactions involving helix-11 that would normally hold the AF2 helix in the conformation permissive for binding coactivators. None of the ERβ structures published to date have shown the AF2 helix in the active position, even though two of the compounds lack any protruding side chain that would necessarily displace the AF2 helix. To understand this dichotomy, we built a three-dimensional model for the activated form of ERβ using the ERα/DES structure[43] as a template. This model showed no interactions that would prevent the AF2 helix from assuming the active position. However, graphical comparison with the ERα/DES structure indicated that the interactions holding the ERβ AF2 helix in the active position are weaker than the corresponding interactions in ERα. For example, in ERα, Lys529 and Asp545 form a salt bridge that holds the AF2 helix in the active position while Asn348 and Tyr537 make a hydrogen bond that has a similar effect. Asp545 is mutated to Asn496 in ERβ, replacing the salt bridge with a weaker hydrogen bond, while Asn348 is mutated to Lys300 in ERβ, eliminating the hydrogen bond. These weakened interactions may leave the ERβ helix more free to shift into the coactivator binding site, accounting for the lower levels of activation and higher degree of antagonism observed with ERβ relative to that of ERα.

Conclusion

In this report we have identified a novel series of 1,3,5-triazine-based estrogen receptor (ER) modulators that are modestly selective for the ERβ subtype. The more potent and selective analogues in this series have binding affinities of 10−40 nM at ERβ and selectivity over ERα of up to 30-fold. These compounds function as antagonists at ERβ and weak partial agonists at ERα in a cell-based reporter gene assay. In addition, the cellular potency of the analogues tested is similar to binding affinity, which suggests these analogues are able to adequately cross the cell membrane.

We also report the X-ray crystal structure of one of these compounds (**15**) complexed to the ERβ ligand-binding domain. This crystal structure has features similar to other ER/antagonist structures, with the characteristic hydrogen bond between the phenol moiety and Arg346 in ERβ and with a salt bridge between the basic nitrogen of the piperidine ring and Asp303 as seen in other ER antagonist structures. Two of the residues in the binding pocket differ between the two ER subtypes: ERα Leu384, which is mutated to Met336 in ERβ, and ERα Met421, which is mutated to Ile373 in ERβ. The lipophilic *p*-chlorophenyl moiety in **15** fits closely against Ile373 in ERβ but should interact less favorably with the bulkier and slightly more polar Met 421 of ERα. Additionally, the polar NH group on the phenol arm of the triazine appears to make favorable electrostatic interactions with Met336 in ERβ but cannot make favorable interactions with Leu384 in ERα. The differential interactions with these two residues might account for the observed ERβ selectivity. These ligands could serve as useful tools in elucidating the pharmacology associated with subtype-selective modulation of ERβ.

Experimental Section

Chemistry. All commercial chemicals and solvents are reagent grade and were used without further purification unless otherwise specified. The following solvents and reagents have been abbreviated: tetrahydrofuran (THF), ethyl ether (Et_2O), dimethyl sulfoxide (DMSO), ethyl acetate (EtOAc), dichloromethane (DCM), trifluoroacetic acid (TFA), dimethylformamide (DMF), methanol (MeOH). All reactions except those in aqueous media were carried out with the use of standard techniques for the exclusion of moisture. Reactions were monitored by thin-layer chromatography on 0.25 mm silica gel plates (60F-254, E. Merck) and visualized with UV light, iodine vapors, or 5% phosphomolybdic acid in 95% ethanol.

Final compounds were typically purified by flash chromatography on silica gel (E. Merck 40−63 mm), by radial chromatography on a Chromatotron using prepared silica gel plates, or by preparative reverse-phase high-pressure liquid chromatography (RP-HPLC) using a Waters model 3000 Delta Prep equipped with a Delta-pak radial compression cartridge (C-18, 300 Å, 15 μm, 47 mm × 300 mm) as the stationary phase. The mobile phase employed 0.1% aqueous TFA with acetonitrile as the organic modifier. Linear gradients were used in all cases, and the flow rate was 100 mL/min (t_0 = 5 min). Analytical purity was assessed by RP-HPLC using a Hewlett-Packard series 1050 system equipped with a diode array spectrometer (λ = 200−400 nm). The stationary phase was a Keystone Scientific BDS Hypersil C-18 column (5 μm, 4.6 mm × 200 mm). The mobile phase employed 0.1% aqueous TFA with acetonitrile as the organic modifier and a flow rate of 1.0 mL/min (t_0 = 3 min). Analytical data are reported as retention time, t_R, in minutes (% acetonitrile, time, flow rate). ^{1}H NMR spectra were recorded on a Varian VXR-300, a Varian Unity-400, or a Varian Unity-300 instrument. Chemical shifts are reported in parts per million (ppm, δ units). Coupling constants are reported in units of hertz (Hz). Splitting patterns are designated as s, singlet; d, doublet; t, triplet; q, quartet; m, multiplet; b, broad. Low-resolution mass spectra (MS) were recorded on a JEOL JMS-AX505HA, JEOL SX-102, or SCIEX-APIiii spectrometer. High-resolution mass spectra were recorded on an AMD-604 (AMD Electra GmbH) high-resolution double-focusing mass spectrometer (Analytical Instrument Group, Raleigh, NC). Mass spectra were acquired in the positive ion mode under electrospray ionization (ESI) or fast atom bombardment (FAB) methods. Combustion analyses were performed by Atlantic Microlabs, Inc., Norcross, GA.

General Procedure for the Synthesis of Triazine Analogue Intermediates A. A stirred solution of 5.3 g (29.0 mmol) of cyanuric chloride in 200 mL of DCM was cooled to −10 °C. A solution of 1.0 equiv of the appropriate amine or thiol and either 1.0 equiv of Proton Sponge or 1.0 equiv of *N*,*N*′-diisopropylethylamine in 40 mL of DCM was then added dropwise over 20 min to the cyanuric chloride solution. The resulting mixture was allowed to warm to room temperature and stirred 2 h. The reaction mixture was quenched by pouring it into 150 mL of a 5% aqueous citric acid solution and extracting with DCM (2 × 100 mL). The organic layers were combined, dried ($MgSO_4$), and concentrated in vacuo. Purification of the residue was achieved by silica gel flash column chromatography.

General Procedure for the Synthesis of Triazine Analogue Intermediates B. A stirred 0.1 M solution of monosubstituted dichlorotriazine intermediate **A** (Scheme 1) in either THF or DMF was cooled to 0 °C. A solution of 1.2 equiv of *N*,*N*-diisopropylethylamine and 1.1 equiv of the appropriate amine in THF was added dropwise. The resulting mixture was stirred at 0 °C for 5 min after the addition was complete and then allowed to warm to room temperature and stirred for 16 h. The reaction mixture was then poured into brine (100 mL) and extracted with EtOAc (2 × 100 mL). The organic layers were combined, dried ($MgSO_4$), and concentrated in vacuo. Purification of the residue was achieved by silica gel chromatography.

General Procedure for the Synthesis of Triazines 1−56. A stirred 0.1 M solution of disubstituted monochlorotriazine **B** in 2-propanol, CH_3CN, or 1:1 CH_3CN/DMF at room temperature was treated with 2.2 equiv of the appropriate amine. The resulting solution was heated to reflux for 0.5−6 h and then cooled to room temperature. The reaction mixture was poured into 150 mL of a 1:1 mixture of EtOAc and ether and extracted with brine (1 × 150 mL). The organic layer was separated, dried ($MgSO_4$), and concentrated in vacuo. If removal of a Boc group was required, this was carried out by treatment of a stirred solution of the Boc-protected intermediate in 1,4-dioxane at room temperature with an excess of 4 N HCl in 1,4-dioxane. The resulting solution was stirred for 18 h at room temperature and then poured into 200 mL of saturated aqueous $NaHCO_3$ and extracted with EtOAc (2 × 100 mL). The organic layers were combined, dried ($MgSO_4$), and concentrated in vacuo. Final compounds were purified by silica gel flash column chromatography or by salt formation followed by recrystallization.

4-(2-{[4-[(3-Phenylpropyl)amino]-6-(1-piperazinyl)-1,3,5-triazin-2-yl]amino}ethyl)phenol (1). The title compound was prepared from *tert*-butyl 4-{4-chloro-6-[(3-phenylpropyl)-amino]-1,3,5-triazin-2-yl}-1-piperazinecarboxylate and tyramine followed by deprotection as described above. Purification by silica gel flash column chromatography eluting in gradient fashion first with 1:1 hexanes/EtOAc and then with 9:1 chloroform/methanol followed by 4:1 chloroform/methanol afforded a light-tan foam (92%): ^{1}H NMR (CD_3OD, 400 MHz) δ 7.19 (m, 5 H), 7.10 (d, 2 H, J = 8.0), 6.75 (d, 2 H, J = 8.0), 4.12 (m, 2 H), 3.86 (m, 1 H), 3.71 (m, 4 H), 3.34 (m, 6 H), 2.85 (m, 2 H), 2.71 (m, 2 H), 2.02 (m, 2 H); low-resolution MS (ES^+) *m*/*e* 434 (MH^+), 433 (MH); RP-HPLC (Dynamax C-18 25 cm ×

4.1 mm, 10−100% CH_3CN in H_2O with 0.1% TFA buffer, 30 min, 1 mL/min) $t_R = 11.67$ min, 96% purity. Anal. ($C_{24}H_{31}N_7O$) C, H, N.

4-[2-({4-(4-Methyl-1-piperazinyl)-6-[(3-phenylpropyl)-amino]-1,3,5-triazin-2-yl}amino)ethyl]phenol (2). The title compound was prepared from 4-chloro-6-(4-methyl-1-piperazinyl)-*N*-(3-phenylpropyl)-1,3,5-triazin-2-amine and tyramine as described above. Purification by silica gel flash column chromatography and eluting in gradient fashion first with 1:1 hexanes/EtOAc and then 9:1 chloroform/methanol afforded a cream solid (76%): ^{1}H NMR (CD_3OD, 400 MHz) δ 7.19 (m, 5 H), 7.11 (d, 2 H, $J = 8.3$), 6.73 (d, 2 H, $J = 8.4$), 4.10 (m, 2 H), 3.83 (m, 1 H), 3.69 (m, 4 H), 3.38 (m, 6 H), 3.12 (s, 3 H), 2.82 (m, 2 H), 2.74 (m, 2 H), 1.97 (m, 2 H); low-resolution MS (ES^+) *m/e* 448 (MH^+), 447 (MH); RP-HPLC (Dynamax C-18 25 cm × 4.1 mm, 10−100% CH_3CN in H_2O with 0.1% TFA buffer, 30 min, 1 mL/min) $t_R = 11.31$ min, 98% purity. Anal. ($C_{25}H_{33}N_7O$) C, H, N.

6-({4-(4-Methyl-1-piperazinyl)-6-[(3-phenylpropyl)amino]-1,3,5-triazin-2-yl}amino)-5,6,7,8-tetrahydro-2-naphthalenol (7). The title compound was prepared from 6-chloro-4-[(3-phenylpropyl)amino]-1,3,5-triazin-2-yl}amino)-5,6,7,8-tetrahydro-2-naphthalenol and *N*-methylpiperazine as described above. Purification by silica gel flash column chromatography (50% EtOAc/hexanes to 100% EtOAc gradient solution) gave the title compound (0.12 g, 82%) as a white solid: TLC (100% EtOAc) $R_f = 0.17$; low-resolution MS (ES^+) *m/e* 474 (MH^+); RP-HPLC (Dynamax C-18 25 cm × 4.1 mm, 10−100% CH_3CN in H_2O with 0.1% TFA buffer, 30 min, 1 mL/min) $t_R = 13.69$ min, 98% purity. Anal. ($C_{27}H_{35}N_7O$) C, H, N.

4-(2-{[4-{[3-(4-Chlorophenyl)propyl]sulfanyl}-6-(1-piperazinyl)-1,3,5-triazin-2-yl]amino}ethyl)phenol (15). The title compound was prepared from 4-{2-[(4-chloro-6-{[3-(4-chlorophenyl)propyl]sulfanyl}-1,3,5-triazin-2-yl)amino]ethyl}-phenol and *N*-BOC-piperazine followed by deprotection as described above. The oily residue was triturated (ether) to afford the title compound as a white solid (0.47 g, 93%): low-resolution MS (ES^+) *m/e* 485 (MH^+); RP-HPLC (Dynamax C-18 25 cm × 4.1 mm, 5−50% CH_3CN in H_2O with 0.1% TFA buffer, 30 min, 1 mL/min) $t_R = 23.57$ min, 98% purity. Anal. ($C_{24}H_{29}ClN_6OS$) C, H, N.

4-(2-{[4-[[3-(4-Chlorophenyl)propyl](methyl)amino]-6-(1-piperazinyl)-1,3,5-triazin-2-yl]amino}ethyl)phenol (17). The title compound was prepared from *tert*-butyl 4-{4-chloro-6-[[3-(4-chlorophenyl)propyl](methyl)amino]-1,3,5-triazin-2-yl}-1-piperazinecarboxylate and tyramine followed by deprotection as described above. Purification by silica gel flash column chromatography and eluting in gradient fashion first with 1:1 hexanes/EtOAc, then 9:1 chloroform/methanol, and then 4:1 chloroform/methanol afforded a light-tan foam. The HCl salt was prepared by dissolution of the free base in EtOAc and addition of 1 M HCl in ether, followed by filtration of the resulting white precipitate and drying at 80 °C/20 Torr to afford 925 mg (80%) of a white solid: ^{1}H NMR (CD_3OD, 400 MHz) δ 7.25 (m, 4 H), 7.10 (d, 2 H, $J = 8.0$), 6.75 (d, 2 H, $J = 8.4$), 4.12 (m, 2 H), 3.86 (m, 1 H), 3.71 (m, 4 H), 3.34 (m, 6 H), 3.14 (s, 3 H), 2.85 (m, 2 H), 2.71 (m, 2 H), 2.02 (m, 2 H); low-resolution MS (ES^+) *m/e* 483 (MH^+), 482 (MH); RP-HPLC (Dynamax C-18 25 cm × 4.1 mm, 10−100% CH_3CN in H_2O with 0.1% TFA buffer, 30 min, 1 mL/min) $t_R = 12.68$ min, 97% purity. Anal. ($C_{25}H_{32}ClN_7O$·HCl) C, H, N.

4-(2-{[4-[[3-(3,4-difluorophenyl)propyl](methyl)amino]-6-(1-piperazinyl)-1,3,5-triazin-2-yl]amino}ethyl)phenol (24). The title compound was prepared from *tert*-butyl 4-{4-chloro-6-[[3-(3,4-difluorophenyl)propyl](methyl)amino]-1,3,5-triazin-2-yl}-1-piperazinecarboxylate and tyramine followed by deprotection as described above. Purification by silica gel flash column chromatography and eluting with 8:1 chloroform/methanol afforded 35 mg (57%) of a light-tan foam: ^{1}H NMR (CD_3OD, 400 MHz) δ 7.03 (m, 5 H), 6.63 (d, 2 H, $J = 7.0$), 4.02 (m, 4 H), 3.57 (m, 4 H), 3.23 (m, 4 H), 3.05 (s, 3 H), 2.75 (m, 2 H), 2.59 (m, 2 H), 1.91 (m, 2 H); low-resolution MS (ES^+) *m/e* 485 (MH^+), 484 (MH); RP-HPLC (Dynamax C-18 25 cm × 4.1 mm, 10−100% CH_3CN in H_2O with 0.1% TFA buffer, 30 min, 1 mL/min) $t_R = 14.21$ min, 93% purity.

4-(2-{[4-[[3-(2-Chlorophenyl)propyl](methyl)amino]-6-(1-piperazinyl)-1,3,5-triazin-2-yl]amino}ethyl)phenol (25). The title compound was prepared from *tert*-butyl 4-{4-chloro-6-[[3-(2-chlorophenyl)propyl](methyl)amino]-1,3,5-triazin-2-yl}-1-piperazinecarboxylate and tyramine followed by deprotection as described above. Purification by silica gel flash column chromatography and eluting with 8:1 chloroform/methanol afforded 50 mg (82%) of a light-tan foam: ^{1}H NMR (CD_3OD, 400 MHz) δ 7.26 (m, 2 H), 7.14 (m, 2 H), 6.99 (d, 2 H, $J = 8.1$), 6.64 (d, 2 H, $J = 8.1$), 4.03 (m, 4 H), 3.60 (m, 4 H), 3.23 (m, 4 H), 3.07 (s, 3 H), 2.73 (m, 4 H), 1.94 (m, 2 H); low-resolution MS (ES^+) *m/e* 483 (MH^+), 482 (MH); RP-HPLC (Dynamax C-18 25 cm × 4.1 mm, 10−100% CH_3CN in H_2O with 0.1% TFA buffer, 30 min, 1 mL/min) $t_R = 13.22$ min, 95% purity.

4-(2-{[4-[[3-(-{Methyl[(2-phenyl-*cis*-cyclopropyl)-methyl]amino}-6-(1-piperazinyl)-1,3,5-triazin-2-yl]amino}ethyl)-phenol (31). The title compound was prepared from *tert*-butyl 4-{4-chloro-6-{methyl[(2-phenyl-*cis*-cyclopropyl)methyl]amino}-1,3,5-triazin-2-yl)-1-piperazinecarboxylate and tyramine followed by deprotection as described above. Purification by silica gel chromatogrpahy and eluting in gradient fashion first with 7:1 chloroform/MeOH, then 3:1 chloroform/MeOH, and finally 2:1 chloroform/MeOH afforded a yellow oil. The HCl salt was generated by dissolving the oil in chloroform, addition of 1 N HCl in ether, filtration of the resulting yellow precipitate, and drying at 50 °C/20 Torr to afford 29 mg (21%) of a yellow solid: ^{1}H NMR (DMSO-d_6, 400 MHz) δ 9.12 (s, br, 1 H), 7.25 (m, 5 H), 7.03 (d, 2 H, $J = 8.4$), 6.68 (d, 2 H, $J = 8.4$), 3.87 (m, 4 H), 3.64 (m, 4 H), 3.14 (m, 2 H), 2.92, (m,2 H), 2.85 (s, br, 1 H), 2.70 (m, 2 H), 2.50 (s, 3 H), 2.26 (m, 1 H), 1.52 (m, 1 H), 1.23 (m, 2 H); low-resolution MS (ES^+) *m/e* 461 (MH^+), 460 (MH). Anal. ($C_{26}H_{33}N_7O$·HCl) C, H, N.

4-[2-({4-[[2-(4-Chlorophenoxy)ethyl](methyl)amino]-6-[4-(2-hydroxyethyl)piperazin-1-yl]-1,3,5-triazin-2-yl}-amino)ethyl]phenol (39). The title compound was prepared from 6-chloro-N^2-[3-(4-chlorophenyl)propyl]-N^4-[2-(4-methoxyphenyl)ethyl]-N^2-methyl-1,3,5-triazine-2,4-diamine and methyl 2-(1-piperazinyl)ethyl ether via the procedure described for compound **36** to afford 10 mg of the title compound as a yellow oil: ^{1}H NMR ($CDCl_3$, 400 MHz) δ 7.23−7.16 (d, 2 H, $J = 7.4$), 7.12−7.03 (d, 2 H, $J = 7.5$), 7.03−6.96 (d, 2 H, $J = 8.0$), 6.73−6.65 (d, 2 H, $J = 8.1$), 3.92−3.40 (m, 8 H), 3.04 (s, 2 H), 2.84−2.68 (t, 1 H, $J = 6.8$), 2.67−2.40 (m, 10 H), 1.85 (bs, 2 H); TLC (1:10 MeOH/DCM): $R_f = 0.12$; low-resolution MS (ES^+) *m/e* 529 (MH^+); RP-HPLC (Dynamax C-18 25 cm × 4.1 mm, 30−100% CH_3CN in H_2O with 0.1% TFA buffer, 30 min, 1 mL/min) $t_R = 10.12$ min, 95% purity. Anal. ($C_{26}H_{34}N_7O_3Cl$·1.0H_2O) H, N, C: calcd 57.19, found 56.53.

4-{2-[(4-[[3-(4-Chlorophenyl)propyl](methyl)amino]-6-{4-[(2-methyl-1,3-thiazol-4-yl)methyl]-1-piperazinyl}-1,3,5-triazin-2-yl)amino]ethyl}phenol (43). The title compound was prepared in 50% yield via the procedure outlined for **40** using 4-chloromethyl-2-methylthiazole hydrochloride to give an off-white glass: ^{1}H NMR ($CDCl_3$, 400 MHz) δ 7.18 (d, 2 H, $J = 8.0$), 7.10−7.02 (m, 2 H), 6.98−6.95 (m, 3 H), 6.64 (d, 2 H, $J = 8.0$), 3.85−3.45 (m, 10 H), 3.02 (s, 3 H), 2.78−2.68 (m, 5 H), 2.55−2.50 (m, 2 H), 2.50−2.46 (m, 4 H), 1.92−1.80 (m, 2 H); low-resolution MS (ES^+) *m/e* 594 (MH^+); TLC (5:5:1 DCM/EtOAc/MeOH): $R_f = 0.50$. Anal. ($C_{30}H_{37}ClN_8OS$) C, H, N.

Biological Assays. Expression of hERβ LBD. Human ERβ LBD was expressed in *E. coli* strain BL21(DE3) as an amino-terminal polyhistidine tagged fusion protein. Expression was under the control of an IPTG inducible T7 promoter. DNA encoding this recombinant protein was subcloned into the pRSET-A expression vector (Invitrogen, Carlesbad, CA). The encoded sequence of the polyhistidine tag (MKKGHHHHG) was incorporated into the 5′ PCR amplification primer, which was upstream of DNA encoding residues 250−530 of ERβ. The coding sequence of ERβ LBD was derived from GenBank (accession number NM_001437). The resulting complete encoded sequence is as follows:

MKKGHHHHGH APRVRELLLD ALSPEQLVLT LLEAEP-PHVL ISRPSAPFTE ASMMMSLTKL ADKELVHMIS WAK-KIPGFVE LSLFDQVRLL ESCWMEVLMM GLMWRSIDHP

GKLIFAPDLV LDRDEGKCVE GILEIFDMLL ATTSRFRELK LQHKEYLCVK AMILLNSSMY PLVTATQDAD SSRKLAHLLN AVTDALVWVI AKSGISSQQQ SMRLANLLML LSHVRHASNK GMEHLLNMKC KNVVPVYDLL LEMLNAHVLR GCKSSITGSE CSPAEDSKSK EGSQNPQSQ

Ten-liter fermentation batches were grown in LB media with 0.1 mg/mL ampicillin at 22 °C for 16 h until $OD_{600} = 14$. At this cell density, 0.25 mM IPTG was added and induction proceeded for 4 h to a final $OD_{600} = 16$. Cells were harvested by centrifugation (20 min, 3500 g, 4 °C), and concentrated cell slurries were stored in PBS at −80 °C.

Purification of ERβ LBD. An amount of 30−40 g of cell paste (equivalent to 2−3 L of the fermentation batch) was resuspended in 300−400 mL of TBS, pH 8.0 (25mM Tris, 150 mM NaCl). Cells were lysed by passing three times through a homogenizer (Rannie), and cell debris was removed by centrifugation (30 min, 20000*g*, 4 °C). The cleared supernatant was filtered through coarse prefilters, and TBS, pH 8.0, containing 500 mM imidazole was added to obtain a final imidazole concentration of 50 mM. This lysate was loaded onto a column (6 cm × 8 cm) packed with Sepharose [Ni^{2+}-charged] chelation resin (Amersham Pharmacia Biotech, Piscataway, NJ) and preequilibrated with TBS, pH 8.0, per 50 mM imidazole. After a wash to baseline absorbance with equilibration buffer, the column was developed with a linear gradient of 50−365 mM imidazole in TBS, pH 8.0. Column fractions were pooled and dialyzed against TBS, pH 8.0, containing 5% 1,2-propanediol, 5 mM DTT, and 0.5 mM EDTA. The protein sample was concentrated using Centri-prep 10K (Amicon, Beverly, MA) and subjected to size exclusion chromatography using a column (3 cm × 90 cm) packed with Sepharose S-75 resin (Amersham Pharmacia Biotech) preequilibrated with TBS, pH 8.0, containing 5% 1,2-propanediol, 5 mM DTT, and 0.5 mM EDTA.

Biotinylation of ERβ LBD. Purified ERβ LBD was buffer-exchanged using PD-10 gel filtration columns into PBS [100 mM Na phosphate, pH 7.2, 150 mM NaCl]. The LBD was diluted to approximately 30 μM in PBS, and a 5-fold molar excess of NHS-LC-biotin (Pierce) was added in a minimal volume of PBS. This solution was incubated with gentle mixing for 60 min at ambient room temperature. The biotinylation modification reaction was stopped by the addition of 2000× molar excess of Tris-HCl, pH 8.0. The modified LBD was dialyzed against two buffer changes, each of at least 50 volumes: TBS, pH 8.0, containing 5 mM DTT, 2 mM EDTA and 2% sucrose. This modified protein was distributed into aliquots, frozen on dry ice, and stored at −80 °C. The biotinylated LBD was subjected to mass spectrometric analysis to reveal the extent of modification by the biotinylation reagent. In general, approximately 95% of the protein had at least a single site of biotinylation, and the overall extent of biotinylation followed a normal distribution of multiple sites, ranging from one to seven.

Radioligand Binding Assays. Ligand binding to purified human ERβ ligand binding domain was measured using scintillation proximity assay similar to that described for PPARγ.[26] A sample of 5 nM of biotinylated ERβ was immobilized on 5 mg/mL streptavidin scintillation proximity beads and incubated for 30 min. The slurry was then centrifuged and resuspended in the appropriate amount of assay buffer. Each assay well contained receptor-coated beads, 1 nM [^{3}H]-17β-estradiol, and the desired concentration of test compound(s) or controls. In general, the total volume was held constant by varying the concentration and volume of radioligand to compensate for any changes in the volume of a particular set of samples, whereas the concentration and volume of receptor-coated bead stock were held constant. The plates were incubated for at least 1 h at room temperature, and bound radioactivity for each well was determined in a Wallac 1450 micro-β counter. The data were analyzed as previously described.[26] Binding assays using crude ERα and ERβ proteins were conducted via a scintillation proximity assay using a bacterial lysate containing overexpressed GST-hERα or GST-hERβ ligand binding domain. Yttrium silicate SPA beads were suspended in assay buffer and dispensed at 0.5 mg/well. For competition binding assays, lysates containing GST-hERα or GST-hERβ were diluted in assay buffer and added to plates to give a final concentration of ∼0.15−0.2 μg of protein with a final assay volume of 100 μL. Test compounds were dissolved in DMSO, serially diluted in assay buffer, and added to the wells in 10 μL aliquots. A sample of 1 nM [^{3}H]-17β-estradiol was then added and the plates were shaken for 2 h before radioactivity was counted.

Cell-Based Functional Assay. Transcriptional activity was measured in a human breast cancer cell line (T47D) transfected with full-length hERα or hERβ and an estrogen-responsive reporter gene construct (ERE)2-tk-SPAP, consisting of two copies of an estrogen receptor response element, the estrogen-responsive HSV tk promoter, and the secreted placental alkaline phosphatase reporter gene. T47D cells were plated at a density of 20 000 cells per well in phenol red free high glucose DMEM supplemented with 10% charcoal/dextran-treated FBS. Transfection mixes contained 4 ng of receptor expression vector, 8 ng of reporter plasmid, 25 ng of β-galactosidase expression vector as internal control, and 43 ng of carrier plasmid. Transfections were performed with Lipofectamine Plus according to the manufacturer's instructions. Drug dilutions were prepared in phenol red free DMEM/F-12 with 15 mM HEPES supplemented with 10% charcoal-stripped, delipidated calf serum that had been heat-inactivated at 62 °C for 35 min. Cells were incubated for 24 h in the presence of drugs, after which the medium was sampled and assayed for SPAP activity. β-Galactosidase activity was determined by using 3.6 mM *o*-nitrophenyl-β-D-galactopyranoside in 0.1 M sodium phosphate pH 7.2 buffer containing 0.13% Triton X-100 as substrate.

Supporting Information Available: X-ray crystallographic data, synthetic procedures, and analytical data for preparation of intermediates; synthetic procedures and analytical data for preparation of final compounds not listed in Experimental Section; and HPLC purity data on final compounds. This material is available free of charge via the Internet at http://pubs.acs.org.

References

(1) Cosman, F.; Lindsay, R. Selective estrogen receptor modulators: clinical spectrum. *Endocr. Rev.* **1999**, *20*, 418−434.
(2) Barrett-Connor, E.; Cox, D. A.; Anderson, P. W. The Potential of SERMs for Reducing the Risk of Coronary Heart Disease. *Trends Endocrinol. Metab.* **1999**, *10*, 320−325.
(3) Yaffe, K.; Sawaya, G.; Lieberburg, I.; Grady, D. Estrogen therapy in postmenopausal women: effects on cognitive function and dementia. *JAMA, J. Am. Med. Assoc.* **1998**, *279*, 688−695.
(4) Zumoff, B. Does postmenopausal estrogen administration increase the risk of breast cancer? Contributions of animal, biochemical, and clinical investigative studies to a resolution of the controversy. *Proc. Soc. Exp. Biol. Med.* **1998**, *217*, 30−37.
(5) Beresford, S. A.; Weiss, N. S.; Voigt, L. F.; McKnight, B. Risk of endometrial cancer in relation to use of oestrogen combined with cyclic progestagen therapy in postmenopausal women. *Lancet* **1997**, *349*, 458−461.
(6) Grese, T. A.; Dodge, J. A. Selective estrogen receptor modulators (SERMs). *Curr. Pharm. Des.* **1998**, *4*, 71−92.
(7) Lin, X.; Huebner, V. Non-steroidal ligands for steroid hormone receptors. *Curr. Opin. Drug Discovery Dev.* **2000**, *3*, 383−398.
(8) McDonnell, D. P. The molecular pharmacology of SERMs. *Trends Endocrinol. Metab.* **1999**, *10*, 301−311.
(9) Kuiper, G. G. J. M.; Enmark, E.; Pelto-Huikko, M.; Nilsson, S.; Gustafsson, J.-A. Cloning of a novel estrogen receptor expressed in rat prostate and ovary. *Proc. Natl. Acad. Sci. U.S.A.* **1996**, *93*, 5925−5930.
(10) Mosselman, S.; Polman, J.; Dijkema, R. ERβ: identification and characterization of a novel human estrogen receptor. *FEBS Lett.* **1996**, *392*, 49−53.
(11) Kuiper, G. G. J. M.; Gustafsson, J.-A. The novel estrogen receptor-β subtype: potential role in the cell- and promoter-specific actions of estrogens and anti-estrogens. *FEBS Lett.* **1997**, *410*, 87−90.
(12) Kuiper, G. G. J. M.; Carlsson, B.; Grandien, K.; Enmark, E.; Haeggblad, J.; et al. Comparison of the ligand binding specificity and transcript tissue distribution of estrogen receptors α and β. *Endocrinology* **1997**, *138*, 863−870.

(13) Hewitt, S. C.; Couse, J. F.; Korach, K. S. Estrogen receptor transcription and transactivation. Estrogen receptor knockout mice: what their phenotypes reveal about mechanisms of estrogen action. *Breast Cancer Res.* **2000**, *2*, 345−352.
(14) Couse, J. F.; Korach, K. S. Estrogen receptor null mice: what have we learned and where will they lead us? *Endocr. Rev.* **1999**, *20*, 358−417.
(15) Dupont, S.; Krust, A.; Gansmuller, A.; Dierich, A.; Chambon, P.; et al. Effect of single and compound knockouts of estrogen receptors α (ERα) and β (ERβ) on mouse reproductive phenotypes. *Development* **2000**, *127*, 4277−4291.
(16) Barkhem, T.; Carlsson, B.; Nilsson, Y.; Enmark, E.; Gustafsson, J.-A.; et al. Differential response of estrogen receptor α and estrogen receptor β to partial estrogen agonists/antagonists. *Mol. Pharmacol.* **1998**, *54*, 105−112.
(17) Meyers, M. J.; Sun, J.; Carlson, K. E.; Katzenellenbogen, B. S.; Katzenellenbogen, J. A. Estrogen Receptor Subtype-Selective Ligands: Asymmetric Synthesis and Biological Evaluation of *cis*- and *trans*-5,11-Dialkyl-5,6,11,12-tetrahydrochrysenes. *J. Med. Chem.* **1999**, *42*, 2456−2468.
(18) Stauffer, S. R.; Coletta, C. J.; Tedesco, R.; Nishiguchi, G.; Carlson, K.; et al. Pyrazole Ligands: Structure−Affinity/Activity Relationships and Estrogen Receptor-α Selective Agonists. *J. Med. Chem.*, **2000**, *43*, 4934−4947.
(19) Stauffer, S. R.; Sun, J.; Katzenellenbogen, B. S.; Katzenellenbogen, J. A. Acyclic amides as estrogen receptor ligands: Synthesis, binding, activity and receptor interaction. *Bioorg. Med. Chem.* **2000**, *8*, 1293−1316.
(20) Sun, J.; Meyers, M. J.; Fink, B. E.; Rajendran, R.; Katzenellenbogen, J. A.; et al. Novel ligands that function as selective estrogens or antiestrogens for estrogen receptor-α or estrogen receptor-β. *Endocrinology* **1999**, *140*, 800−804.
(21) Schopfer, U.; Schoeffter, P.; Bischoff, S. F.; Nozulak, J.; Feuerbach, D.; et al. Toward Selective ERβ Agonists for Central Nervous System Disorders: Synthesis and Characterization of Aryl Benzthiophenes. *J. Med. Chem.* **2002**, *45*, 1399−1401.
(22) Meyers, M. J.; Sun, J.; Carlson, K. E.; Marriner, G. A.; Katzenellenbogen, B. S.; et al. Estrogen Receptor-β Potency-Selective Ligands: Structure−Activity Relationship Studies of Diarylpropionitriles and Their Acetylene and Polar Analogues. *J. Med. Chem.* **2001**, *44*, 4230−4251.
(23) Masquelin, T.; Meunier, N.; Gerber, F.; Rosse, G. Solution- and solid-phase synthesis of combinatorial libraries of trisubstituted 1,3,5-triazines. *Heterocycles* **1998**, *48*, 2489−2505.
(24) Scharn, D.; Wenschuh, H.; Reineke, U.; Schneider-Mergener, J.; Germeroth, L. Spatially Addressed Synthesis of Amino- and Amino-Oxy-Substituted 1,3,5-Triazine Arrays on Polymeric Membranes. *J. Comb. Chem.* **2000**, *2*, 361−369.
(25) Scharn, D.; Germeroth, L.; Schneider-Mergener, J.; Wenschuh, H. Sequential Nucleophilic Substitution on Halogenated Triazines, Pyrimidines, and Purines: A Novel Approach to Cyclic Peptidomimetics. *J. Org. Chem.* **2001**, *66*, 507−513.
(26) Nichols, J. S.; Parks, D. J.; Consler, T. G.; Blanchard, S. G. Development of a scintillation proximity assay for peroxisome proliferator-activated receptor γ ligand binding domain. *Anal. Biochem.* **1998**, *257*, 112−119.
(27) Mortensen, D. S.; Rodriguez, A. L.; Sun, J.; Katzenellenbogen, B. S.; Katzenellenbogen, J. A. Furans with basic side chains: synthesis and biological evaluation of a novel series of antagonists with selectivity for the estrogen receptor alpha. *Bioorg. Med. Chem. Lett.* **2001**, *11*, 2521−2524.
(28) Henke, B. R.; Drewry, D. H.; Jones, S. A.; Stewart, E. L.; Weaver, S. L.; et al. 2-Amino-4,6-diarylpyridines as novel ligands for the estrogen receptor. *Bioorg. Med. Chem. Lett.* **2001**, *11*, 1939−1942.
(29) Lesuisse, D.; Albert, E.; Bouchoux, F.; Cerede, E.; Lefrancois, J. M.; et al. Biphenyls as surrogates of the steroidal backbone. Part 1: synthesis and estrogen receptor affinity of an original series of polysubstituted biphenyls. *Bioorg. Med. Chem. Lett.* **2001**, *11*, 1709−1712.
(30) Endo, Y.; Iijima, T.; Yamakoshi, Y.; Fukasawa, H.; Miyaura, C.; et al. Potent estrogen agonists based on carborane as a hydrophobic skeletal structure: a new medicinal application of boron clusters. *Chem. Biol.* **2001**, *8*, 341−355.
(31) Tedesco, R.; Youngman, M. K.; Wilson, S. R.; Katzenellenbogen, J. A. Synthesis and evaluation of hexahydrochrysene and tetrahydrobenzofluorene ligands for the estrogen receptor. *Bioorg. Med. Chem. Lett.* **2001**, *11*, 1281−1284.
(32) Stauffer, S. R.; Huang, Y.; Coletta, C. J.; Tedesco, R.; Katzenellenbogen, J. A. Estrogen pyrazoles: defining the pyrazole core structure and the orientation of substituents in the ligand binding pocket of the estrogen receptor. *Bioorg. Med. Chem.* **2001**, *11*, 141−150.
(33) Miller, C. P.; Collini, M. D.; Tran, B. D.; Harris, H. A.; Kharode, Y. P.; et al. Design, Synthesis, and Preclinical Characterization of Novel, Highly Selective Indole Estrogens. *J. Med. Chem.* **2001**, *44*, 1654−1657.
(34) Minutolo, F.; Bertini, S.; Papi, C.; Carlson, K. E.; Katzenellenbogen, J. A.; et al. Salicylaldoxime Moiety as a Phenolic "A-Ring" Substitute in Estrogen Receptor Ligands. *J. Med. Chem.* **2001**, *44*, 4288−4291.
(35) Nishiguchi, G. A.; Rodriguez, A. L.; Katzenellenbogen, J. A. Diaryl-dialkyl-substituted pyrazoles: regioselective synthesis and binding affinity for the estrogen receptor. *Bioorg. Med. Chem. Lett.* **2002**, *12*, 947−950.
(36) Sun, J.; Huang, Y. R.; Harrington, W. R.; Sheng, S.; Katzenellenbogen, J. A.; et al. Antagonists selective for estrogen receptor α. *Endocrinology* **2002**, *143*, 941−947.
(37) Anstead, G. M.; Carlson, K. E.; Katzenellenbogen, J. A. The estradiol pharmacophore: ligand structure−estrogen receptor binding affinity relationships and a model for the receptor binding site. *Steroids* **1997**, *62*, 268−303.
(38) Brzozowski, A. M.; Pike, A. C. W.; Dauter, Z.; Hubbard, R. E.; Bonn, T.; et al. Molecular basis of agonism and antagonism in the estrogen receptor. *Nature* **1997**, *389*, 753−758.
(39) Wurtz, J.-M.; Egner, U.; Heinrich, N.; Moras, D.; Mueller-Fahrnow, A. Three-Dimensional Models of Estrogen Receptor Ligand Binding Domain Complexes, Based on Related Crystal Structures and Mutational and Structure−Activity Relationship Data. *J. Med. Chem.* **1998**, *41*, 1803−1814.
(40) Pike, A. C. W.; Brzozowski, A. M.; Hubbard, R. E.; Bonn, T.; Thorsell, A.-G.; et al. Structure of the ligand-binding domain of oestrogen receptor beta in the presence of a partial agonist and a full antagonist. *EMBO J.* **1999**, *18*, 4608−4618.
(41) Egner, U.; Heinrich, N.; Ruff, M.; Gangloff, M.; Mueller-Fahrnow, A.; et al. Different ligands−different receptor conformations: modeling of the hERα LBD in complex with agonists and antagonists. *Med. Res. Rev.* **2001**, *21*, 523−539.
(42) Tanenbaum, D. M.; Wang, Y.; Williams, S. P.; Sigler, P. B. Crystallographic comparison of the estrogen and progesterone receptor's ligand binding domains. *Proc. Natl. Acad. Sci. U.S.A.* **1998**, *95*, 5998−6003.
(43) Shiau, A. K.; Barstad, D.; Loria, P. M.; Cheng, L.; Kushner, P. J.; et al. The structural basis of estrogen receptor/coactivator recognition and the antagonism of this interaction by tamoxifen. *Cell* **1998**, *95*, 927−937.
(44) Matthews, J.; Celius, T.; Halgren, R.; Zacharewski, T. Differential estrogen receptor binding of estrogenic substances: a species comparison. *J. Steroid Biochem. Mol. Biol.* **2000**, *74*, 223−234.
(45) Sanderson, J. T.; Seinen, W.; Giesy, J. P.; Van den Berg, M. 2-Chloro-*s*-triazine herbicides induce aromatase (CYP19) activity in H295R human adrenocortical carcinoma cells: a novel mechanism for estrogenicity? *Toxicol. Sci.* **2000**, *54*, 121−127.
(46) Sanderson, J. T.; Letcher, R. J.; Heneweer, M.; Giesy, J. P.; Van den Berg, M. Effects of chloro-*s*-triazine herbicides and metabolites on aromatase activity in various human cell lines and on vitellogenin production in male carp hepatocytes. *Environ. Health Perspect.* **2001**, *109*, 1027−1031.
(47) Klinge, C. M. Estrogen receptor interaction with estrogen response elements. *Nucleic Acids Res.* **2001**, *29*, 2905−2919.
(48) Foster, A. B.; Jarman, M.; Leung, O. T.; McCague, R.; Leclercq, G.; et al. Hydroxy derivatives of tamoxifen. *J. Med. Chem.* **1985**, *28*, 1491−1497.
(49) Grese, T. A.; Cho, S.; Finley, D. R.; Godfrey, A. G.; Jones, C. D.; et al. Structure−Activity Relationships of Selective Estrogen Receptor Modulators: Modifications to the 2-Arylbenzothiophene Core of Raloxifene. *J. Med. Chem.* **1997**, *40*, 146−167.
(50) Lambert, M. H. Docking conformationally flexible molecules into protein binding sites. In *Practical Application of Computer-Aided Drug Design*; Charifson, P. S., Ed.; Marcel Dekker: New York, 1997; Chapter 8, pp 243−303.
(51) Insight II is available from Accelrys, Inc., San Diego, CA 92121.
(52) Pike, A. C. W.; Brzozowski, A. M.; Walton, J.; Hubbard, R. E.; Thorsell, A.-G.; et al. Structural insights into the mode of action of a pure antiestrogen. *Structure* **2001**, *9*, 145−153.
(53) Shiau, A. K.; Barstad, D.; Radek, J. T.; Meyers, M. J.; Nettles, K. W.; et al. Structural characterization of a subtype-selective ligand reveals a novel mode of estrogen receptor antagonism. *Nat. Struct. Biol.* **2002**, *9*, 359−364.

JM020291H